

Fig. 5. Charge densities of (I) computed by the CNDO/2 method. Vibrational ellipsoids are at the 50% probability level (Johnson, 1965).

unique conformation does not involve such an interaction. As a result of this repulsive interaction, a rotation of the pyridine plane around N(1)—C(8) by  $14.8^\circ$  (Table 7) and an in-plane deformation [ $N(1)C(8)C(12) = 124.7^\circ$ ] occur to give a separation of  $2.0 \text{ \AA}$  for  $H(C7)\cdots H(C12)$ . However, the small deviation from planarity does not seem to prevent the close parallel packing of the molecules along the shortest axis with an interplanar distance of  $3.44 \text{ \AA}$ .

The rest of (I) presents the same features as salicylidene-2-aminopyridines: short C(3)—C(4), C(5)—C(6), C(2)—O(1) bond lengths, due to a quinoid resonance structure, and essentially identical distances for the imino C(7)—N(1) bond as well as C(1)—C(7). The distance  $1.448 \text{ \AA}$  for the latter is in agreement with the partial double-bond character of a formal single bond between an aromatic and a double or a triple bond (Mavridis & Moustakali-Mavridis, 1977, and references therein).

Fig. 5 shows the charge distribution of (I) calculated by the CNDO/2 method (Pople & Beveridge, 1970). The geometry used is that of the present analysis. As

has been observed in our previous studies of salicylidene-2-aminopyridines, there is a strong intramolecular hydrogen bond from the hydroxylic H(O1) to the imino N(1) atom. Assuming that the main cause of the hydrogen bond is electrostatic in origin, a value of  $\sim 25 \text{ kJ mol}^{-1}$  is obtained from the CNDO/2 charges.

We thank Dr D. L. Ward for his help during data collection, and the Chemistry Department of Michigan State University for the use of the diffractometric facilities.

#### References

- BREGMAN, J., LEISEROWITZ, L. & OSAKI, K. (1964). *J. Chem. Soc.* pp. 2086–2100.
- BUSING, W. R., MARTIN, K. O. & LEVY, H. A. (1962). *ORFLS*. Report ORNL-TM-305. Oak Ridge National Laboratory, Tennessee.
- DOYLE, P. A. & TURNER, P. S. (1968). *Acta Cryst.* **A24**, 390–397.
- JOHNSON, C. K. (1965). *ORTEP*. Report ORNL-3794. Oak Ridge National Laboratory, Tennessee.
- LONG, R. E. (1965). PhD Thesis, Univ. of California, Los Angeles.
- MAVRIDIS, A. & MOUSTAKALI-MAVRIDIS, I. (1977). *Acta Cryst.* **B33**, 3612–3615.
- MOUSTAKALI-MAVRIDIS, I., HADJOUJIS, E. & MAVRIDIS, A. (1978). *Acta Cryst.* **B34**, 3709–3715.
- POPLE, J. A. & BEVERIDGE, D. L. (1970). *Approximate Molecular-Orbital Theory*. New York: McGraw-Hill.
- STEWART, R. F., DAVIDSON, E. R. & SIMPSON, W. T. (1965). *J. Chem. Phys.* **42**, 3175–3187.
- VOGEL, A. I. (1966). *Practical Organic Chemistry*, pp. 653–654. London: Longmans.
- WEI, K.-T. & WARD, D. L. (1976). *Acta Cryst.* **B32**, 2768–2773.
- WILSON, A. J. C. (1942). *Nature (London)*, **150**, 151–152.

*Acta Cryst.* (1980). **B36**, 1130–1136

## Neutron Structural Refinement for Pyridoxinium Chloride, a Component $C_8H_{12}ClNO_3$ of the Vitamin $B_6$

BY G. E. BACON AND J. S. PLANT\*

*Department of Physics, The University, Sheffield S10 2TN, England*

(Received 9 August 1979; accepted 24 December 1979)

### Abstract

The structure of pyridoxinium chloride, a constituent of the vitamin  $B_6$ , has been re-investigated using high-flux

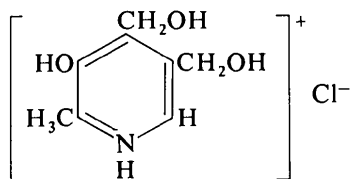
\* Latterly at the Computer Services Department, Sheffield City Polytechnic, but now at the Computer Centre, The University, Keele.

measurements of neutron intensity diffracted by a small single crystal. Re-determined triclinic  $P\bar{1}$  cell ( $Z = 2$ ) constants,  $a = 9.68 (2)$ ,  $b = 5.83 (1)$ ,  $c = 9.54 (2) \text{ \AA}$ ,  $\alpha = 93.88 (8)$ ,  $\beta = 115.06 (5)$ ,  $\gamma = 98.53 (7)^\circ$ , differ from reported values by 1.7% for  $a$ . Least-squares refinement ( $R = 3.6\%$ ) of the structure, using neutron data, produces  $1.012 (9) \text{ \AA}$  for the O(2)—H(12) bond

length: this contrasts with 0.79 (6) Å assessed by Hanic [*Chem. Zvesti* (1968), **22**, 838–843] using X-rays. Joint appraisal of the X-ray and neutron data indicates that this discrepancy for O(2)–H(12) may arise from an electron deficit for H(12). On the other hand, surfeits of electron density occur at the mid-points of most bonds and near the electronegative O and Cl atoms. One CH<sub>2</sub>OH group of the structure is rotated 16° from the molecular plane, such that its oxygen atom O(1), is displaced 0.32 Å from the plane of the pyridine ring, with which another CH<sub>2</sub>OH group is almost coplanar. Rigid-body analyses indicate that the former CH<sub>2</sub>OH group librates less (6° r.m.s.) than its freer counterpart (9° r.m.s.), whilst CH<sub>3</sub> librates by 25° r.m.s.: the largest component of thermal motion is normal to flat strip-like chains of adjoining molecules, with the molecular cores librating most (5° r.m.s.) about an axis which lies across the flat strips.

### Introduction

An exceptionally short O–H bond length 0.79 (6) Å was reported by Hanic (1966, 1968) for pyridoxinium chloride, elsewhere termed pyridoxine hydrochloride,



a component of the vitamin B<sub>6</sub>. Hanic's X-ray measurement derives from difference-Fourier determination and least-squares refinement of hydrogen electron positions and concerns a hydrogen atom that is involved in both intermolecular and intramolecular bonding (Fig. 1). In

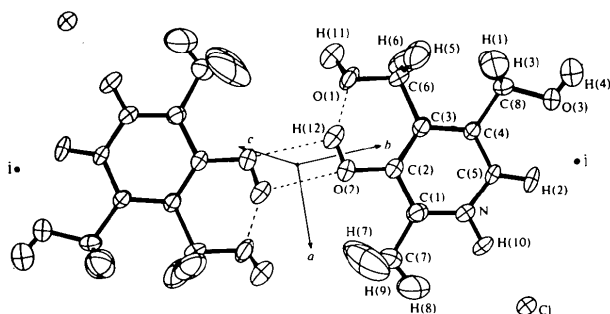


Fig. 1. O...H bonding forming a bimolecular complex in pyridoxinium chloride. Atoms are designated by 50% probability ellipsoids, as drawn by ORTEP (Johnson, 1970). The directions of the crystallographic axes are indicated by drawn lines, with lengths  $a/4$ ,  $b/2$ ,  $c/4$ . The  $b$  and  $c$  axes are inclined steeply upwards from the plane of the page, at 35 and 45° respectively, whilst the  $a$  axis is tilted slightly (8°) downwards, away from the reader.

the present work, the structure of this compound has been re-investigated using neutron diffraction techniques, in an experiment that has served to establish the smallest size of crystal that may be examined successfully with high-flux neutron beams at the ILL, Grenoble. Single crystals used as samples here are about ten times smaller, 0.6 mm<sup>3</sup>, than ones hitherto required for this type of neutron experiment.

### Experimental details

#### Amended cell dimensions

Crystals were examined by X-ray Weissenberg photographs using Mo  $K\alpha$  radiation. In particular, the value obtained for the cell constant  $a = 9.68$  (2) Å differed substantially from the reported value 9.52 (4) Å (Hanic, 1966). Subsequent neutron measurements on further crystals confirmed the amended cell parameters given in the *Abstract* of this paper.

#### Neutron diffraction

Neutron data were collected finally for a 0.6 mm<sup>3</sup> crystal, measuring 0.6, 1.0 and 0.8 mm between (100), (010) and (001) crystalline faces, on the ILL diffractometer D8, with  $\lambda = 1.207$  Å. Crystals were supplied by Dr Hanic. 1602 independent reflections were measured. The profile of each was examined graphically and 105 reflections were rejected, for such reasons as changing reactor flux during measurement. All reflections were measured for  $\sin \theta/\lambda$  up to 0.475 Å<sup>-1</sup> but only 658 of 743 available reflections in the  $\sin \theta/\lambda$  range 0.475 to 0.586 Å<sup>-1</sup> were measured fully, as peak heights of others were found small when pre-assessed. The  $\bar{1}24$  and  $22\bar{5}$  reflections were used as standards and their intensities were measured after every 12 useful reflections, *i.e.* about ten times per day. Absorption corrections were applied using *ABSORB* from the *XRAY 72* (1972) suite of programs: correction factors ranged from 0.72 to 0.83 for 010 and  $\bar{1}11$  reflections respectively.

Crystallographic refinement was performed with *CRYLSQ* of *XRAY 72*, and also with *LS* of *SHELX 76* (Sheldrick, 1976). These two different crystallographic computer packages gave rise to similar results except that *SHELX 76* led to 50% larger estimates of standard deviations than *XRAY 72*: tabulated e.s.d.'s are the mean of the two derivations. Absorption and extinction corrections and changes of the weighting scheme had little effect on the final results, or on  $R$ . Refinement was continued until the largest shift each cycle, for any parameter, was less than 0.1 of its e.s.d. The *CRYLSQ* refinement was commenced from the coordinates of Hanic (1968), with assumed isotropic temperature factors  $B = 4.8$  Å<sup>2</sup> for the hydrogen

atoms. An initial  $R(F)$  factor of 28.5 became 14.3% after three cycles of refinement and then 4.0% after allowing for anisotropic temperature factors – this increased the number of variable parameters to 226. The  $R(wF)$  factor was eventually reduced to 3.5% after allowing for effects of absorption and extinction and omitting 215 reflections that were both calculated and measured to be weaker than three times the estimated error  $\sigma(F)$ , mostly statistical, in their measured strength. No more than a half-dozen of the strongest reflections were significantly affected by extinction, with an extinction factor  $(|F_c| - |F_o|)/|F_c|$  limited to 1% for the strongest reflection  $\bar{1}24$ .\*

### Results and discussion

Table 1 lists final fractional coordinates, with standard deviations estimated from the neutron least-squares refinement process. Atoms are numbered in the manner of Hanic (1968) as indicated in Fig. 1. The notation for the thermal parameters, which are also included in

\* A list of structure factors has been deposited with the British Library Lending Division as Supplementary Publication No. SUP 35073 (8 pp.). Copies may be obtained through The Executive Secretary, International Union of Crystallography, 5 Abbey Square, Chester CH1 2HU, England.

Table 1, is given by the Debye–Waller amplitude expression,  $\exp(-B \sin^2 \theta/\lambda^2) = \exp\{-2\pi^2(U_{11}a^{*2}h^2 + U_{22}b^{*2}k^2 + U_{33}c^{*2}l^2 + 2U_{12}a^*b^*hk + 2U_{23}b^*c^*kl + 2U_{31}c^*a^*lh)\}$ , such that  $U_{ij}$  represents a product of mean atomic displacements along  $i$  and  $j$  axes of the structure. Fig. 1 shows a view of the thermal motion of atoms in the pyridoxinium and chlorine ions. It appears that the largest component of the motion is normal to the molecular plane.

### Structural geometry

Fig. 1 illustrates that pairs of pyridoxinium ions are bonded by  $O(2^I)–H(12^I)\cdots O(2^{II})$  to form bimolecular dimers. These dimers are arranged into strip-like chains: successive dimers along a strip are joined through adjacent  $H(10^I)\cdots Cl^I\cdots H(4^{III})$  and  $H(4^I)\cdots Cl^{III}\cdots H(10^{III})$  links, whilst  $Cl^I\cdots H(11^{IV})$  forms diagonal links to parallel chains. Each individual strip is quite flat, except for a few peripheral atoms and a slight stepping between successive molecules along the chain, equalling 0.03 Å at the Cl linkage and 0.21 Å at the centre of the bimolecular pair. The lateral stepping between adjacent strips is much greater, 1.52 Å, arising from an 8° tilt of each strip to the  $a$  axis (see Fig. 1).

Bond lengths are listed in Table 2. The first column of values in this table represents bond lengths reported by Hanic (1966, 1968). It can be contrasted with the second column of values, which represent bond lengths

Table 1. *Atomic parameters derived from neutron structural refinement (uncorrected for librations)*

Fractional coordinates are multiplied by  $10^4$  and thermal parameters are listed in units of  $10^{-3}$  Å<sup>2</sup>.

	$x$	$y$	$z$	$U_{11}$	$U_{22}$	$U_{33}$	$U_{12}$	$U_{13}$	$U_{23}$
Cl	4534 (2)	3298 (4)	2051 (3)	28 (1)	41 (1)	51 (1)	5 (1)	20 (1)	19 (1)
O(1)	-2586 (4)	-2809 (7)	3681 (5)	39 (2)	46 (3)	47 (2)	-4 (2)	23 (2)	18 (2)
O(2)	175 (5)	-3330 (7)	4097 (5)	41 (2)	51 (3)	61 (3)	10 (2)	28 (2)	33 (2)
O(3)	-2000 (5)	4093 (8)	-41 (6)	46 (2)	61 (3)	78 (3)	20 (2)	34 (2)	48 (3)
N	1568 (2)	955 (4)	2323 (3)	25 (1)	38 (1)	40 (1)	4 (1)	17 (1)	13 (1)
C(1)	1541 (3)	-808 (5)	3144 (4)	26 (1)	34 (2)	31 (2)	4 (1)	13 (1)	6 (1)
C(2)	131 (4)	-1591 (6)	3234 (4)	30 (1)	33 (2)	33 (2)	3 (1)	17 (1)	11 (1)
C(3)	-1165 (3)	-587 (5)	2473 (3)	28 (1)	27 (2)	28 (1)	1 (1)	14 (1)	6 (1)
C(4)	-1041 (3)	1239 (5)	1607 (4)	27 (1)	27 (2)	33 (2)	4 (1)	17 (1)	8 (1)
C(5)	349 (4)	1987 (6)	1569 (4)	32 (1)	30 (2)	42 (2)	1 (1)	22 (1)	15 (1)
C(6)	-2709 (4)	-1423 (6)	2496 (4)	28 (1)	43 (2)	46 (2)	5 (1)	21 (1)	13 (2)
C(7)	2947 (4)	-1830 (7)	3903 (4)	32 (1)	55 (3)	41 (2)	11 (2)	12 (1)	13 (2)
C(8)	-2410 (4)	2380 (6)	734 (4)	31 (1)	37 (2)	48 (2)	12 (1)	24 (1)	13 (2)
H(1)	-3376 (8)	1022 (15)	-50 (11)	43 (4)	52 (5)	98 (6)	6 (5)	7 (4)	15 (4)
H(2)	540 (7)	3369 (13)	916 (8)	51 (4)	59 (5)	68 (4)	6 (4)	36 (3)	42 (4)
H(3)	-2770 (10)	3130 (16)	1584 (10)	94 (6)	82 (6)	77 (6)	45 (5)	66 (5)	21 (5)
H(4)	-2841 (8)	4787 (14)	-619 (8)	62 (4)	58 (5)	70 (5)	18 (4)	32 (4)	28 (4)
H(5)	-3156 (10)	106 (15)	2710 (12)	96 (6)	60 (6)	145 (8)	39 (5)	99 (6)	44 (6)
H(6)	-3508 (7)	-2422 (17)	1350 (8)	42 (4)	110 (7)	49 (4)	-13 (4)	13 (3)	13 (4)
H(7)	2682 (11)	-3636 (19)	3630 (18)	81 (6)	56 (7)	216 (14)	38 (6)	7 (8)	5 (8)
H(8)	3779 (11)	-1264 (26)	3527 (13)	76 (6)	198 (14)	144 (9)	74 (8)	74 (6)	105 (9)
H(9)	3332 (12)	-1719 (27)	5094 (10)	112 (7)	200 (14)	46 (5)	94 (9)	21 (5)	38 (7)
H(10)	2587 (6)	1566 (12)	2232 (7)	38 (3)	54 (4)	70 (4)	6 (3)	38 (3)	25 (4)
H(11)	-3476 (7)	-4057 (13)	3321 (8)	47 (4)	52 (5)	66 (5)	-1 (3)	32 (3)	16 (4)
H(12)	-834 (7)	-3627 (14)	4195 (8)	50 (4)	69 (5)	69 (4)	7 (4)	39 (4)	33 (4)

Table 2. Bond lengths (Å)

The X-ray values indicate the effect of the present amendment to the crystal cell parameters, whereas neutron values are shown both uncorrected and corrected for molecular libration.

	X-rays Hanic (1966, 1968)	Re-assessed X-ray	Neutron	Neutron libration corrected
N—C(1)	1.345 (5)	1.343 (6)	1.338 (4)	1.342
N—C(5)	1.325 (5)	1.367 (6)	1.350 (5)	1.355
C(1)—C(2)	1.368 (5)	1.398 (7)	1.414 (5)	1.419
C(2)—C(3)	1.379 (5)	1.408 (7)	1.396 (5)	1.401
C(3)—C(4)	1.409 (5)	1.384 (6)	1.413 (5)	1.417
C(4)—C(5)	1.358 (5)	1.371 (7)	1.368 (5)	1.372
C(1)—C(7)	1.483 (6)	1.493 (8)	1.482 (6)	1.487
C(3)—C(6)	1.490 (5)	1.517 (7)	1.512 (5)	1.517
C(4)—C(8)	1.497 (5)	1.536 (7)	1.514 (5)	1.520
C(2)—O(2)	1.354 (5)	1.345 (6)	1.343 (6)	1.348
C(6)—O(1)	1.435 (5)	1.431 (6)	1.409 (6)	1.413
C(8)—O(3)	1.413 (5)	1.410 (7)	1.390 (7)	1.394
O(1)—H(11)	1.12 (5)	1.50 (6)	0.958 (7)	
O(2)—H(12)	0.79 (6)		1.011 (10)	1.015
O(3)—H(4)	1.03 (6)		0.937 (9)	
N—H(10)	1.17 (6)	1.02 (5)	1.040 (8)	1.043
C(5)—H(2)	1.12 (6)	1.15 (5)	1.092 (9)	1.095
C(6)—H(5)	1.15 (6)		1.090 (11)	1.095
C(6)—H(6)	1.23 (5)	1.15 (6)	1.094 (7)	1.098
C(7)—H(7)	1.14 (5)		1.034 (11)	1.038
C(7)—H(8)	1.13 (4)	1.17 (11)	1.034 (14)	1.038
C(7)—H(9)	1.00 (6)	0.79 (10)	1.029 (10)	1.033
C(8)—H(1)	1.17 (4)	1.17 (6)	1.081 (7)	1.085
C(8)—H(3)	1.14 (6)	1.15 (6)	1.098 (12)	1.103
O(1)⋯H(12)	1.83 (6)		1.706 (9)	
O(2)⋯H(12)	2.47 (6)		2.461 (11)	
Cl⋯H(4)	2.19 (5)		2.157 (8)	
Cl⋯H(10)	1.99 (6)	2.20 (5)	2.082 (8)	
Cl⋯H(11)	1.95 (4)	1.68 (5)	2.108 (7)	

re-determined from Hanic's X-ray data, taking account of our revised crystal cell dimensions. The present neutron results are listed in the third column of Table 2. The fourth column lists the neutron results after correction for effects of thermal libration.

Bond angles appear in Table 3. The N angle C(1)—N—C(5) of the pyridine ring is 124.7 (2), exceeding  $2\pi/3$ , as found also for some other pyridine compounds (Hanic, 1966) — this is attributable to the smaller atomic radius of N as also are shorter measured values (Table 2) for C—N than C—C bonds. Table 4 lists torsion angles: the sign convention is such that an angle  $A(1)—A(2)—A(3)—A(4)$  is positive if there is a clockwise rotation, looking along  $A(2) \rightarrow A(3)$  from  $A(2)—A(1)$  to  $A(3)—A(4)$ .

The two CH<sub>2</sub>OH groups of the pyridoxinium molecule are noticeably different. Thus, O(1)—H(11) of the H<sub>2</sub>COH group that is involved in intramolecular bonding of O(1) to H(12) (Fig. 1) does not lie in the molecular plane: there is a 37.4 (5)° twist of this O—H relative to the C—C link to the pyridine ring and C—O is inclined at 15° to the ring. Furthermore, this H<sub>2</sub>COH

Table 3. Bond angles (°)

	X-ray Hanic (1966, 1968)	Re-assessed X-ray	Neutron
C(1)—N—C(5)	124.5 (3)	123.8 (5)	124.7 (2)
N—C(1)—C(2)	118.1 (3)	117.7 (5)	116.6 (3)
C(1)—C(2)—C(3)	120.1 (3)	120.4 (4)	121.0 (3)
C(2)—C(3)—C(4)	118.8 (3)	118.8 (4)	118.6 (4)
C(3)—C(4)—C(5)	119.6 (3)	120.3 (5)	118.9 (2)
C(4)—C(5)—N	118.9 (3)	119.1 (5)	120.2 (4)
N—C(1)—C(7)	119.4 (3)	119.1 (5)	119.9 (3)
C(2)—C(1)—C(7)	122.5 (3)	123.2 (5)	123.5 (4)
C(1)—C(2)—O(2)	115.8 (3)	115.4 (5)	114.2 (3)
C(3)—C(2)—O(2)	124.1 (3)	124.2 (5)	124.8 (4)
C(2)—C(3)—C(6)	123.0 (3)	122.6 (4)	122.7 (3)
C(4)—C(3)—C(6)	118.2 (3)	118.6 (4)	118.7 (3)
C(3)—C(6)—O(1)	111.7 (3)	112.1 (4)	112.8 (2)
C(3)—C(4)—C(8)	121.4 (3)	121.1 (4)	121.3 (4)
C(5)—C(4)—C(8)	119.0 (3)	118.6 (4)	119.8 (3)
C(4)—C(8)—O(3)	109.5 (3)	108.8 (4)	110.2 (4)
C(6)—O(1)—H(11)	113.6 (2.7)	89.2 (2.0)	110.5 (5)
C(2)—O(2)—H(12)	108.4 (4.0)		108.0 (6)
C(8)—O(3)—H(4)	106.9 (3.5)		111.6 (7)
C(1)—N—H(10)	111.7 (2.7)	109.4 (2.9)	118.4 (4)
C(5)—N—H(10)	122.9 (2.6)	124.5 (3.0)	116.9 (5)
N—C(5)—H(2)	121.6 (2.7)	119.4 (2.8)	116.1 (5)
C(4)—C(5)—H(2)	118.1 (3.0)	117.9 (2.8)	123.7 (5)
C(3)—C(6)—H(5)	108.0 (2.8)		108.5 (6)
C(3)—C(6)—H(6)	105.9 (3.1)	96.8 (3.0)	108.0 (6)
O(1)—C(6)—H(5)	108.9 (3.2)		107.8 (7)
O(1)—C(6)—H(6)	102.4 (2.7)	104.9 (3.2)	110.1 (6)
H(5)—C(6)—H(6)	119.3 (3.3)		109.7 (7)
C(1)—C(7)—H(7)	100.7 (2.6)		111.0 (6)
C(1)—C(7)—H(8)	105.1 (2.7)	93.0 (3.5)	112.0 (8)
C(1)—C(7)—H(9)	99.6 (3.3)	97.9 (6.0)	112.5 (9)
H(7)—C(7)—H(8)	102.4 (2.7)		105.9 (1.3)
H(7)—C(7)—H(9)	92.2 (4.3)		98.2 (1.3)
H(8)—C(7)—H(9)	118.2 (3.6)	167.5 (7.0)	116.1 (9)
O(3)—C(8)—H(1)	104.8 (3.0)	99.3 (3.2)	112.7 (7)
O(3)—C(8)—H(3)	107.6 (2.8)	94.8 (3.1)	111.3 (6)
C(4)—C(8)—H(1)	107.5 (2.8)	107.2 (2.9)	108.2 (5)
C(4)—C(8)—H(3)	111.4 (2.4)	121.3 (3.2)	108.2 (5)
H(1)—C(8)—H(3)	115.9 (3.9)	121.2 (4.5)	106.1 (8)
O(2)—H(12)⋯O(1)	148.3 (5.7)		144.8 (8)
O(2)—H(12)⋯O(2)	101.1 (4.2)		96.3
H(4)⋯Cl⋯H(10)	85.1 (2.1)		80.8
H(4)⋯Cl⋯H(11)	114.8 (2.1)		103.0
H(10)⋯Cl⋯H(11)	144.7 (2.4)	164.6 (2.4)	140.1

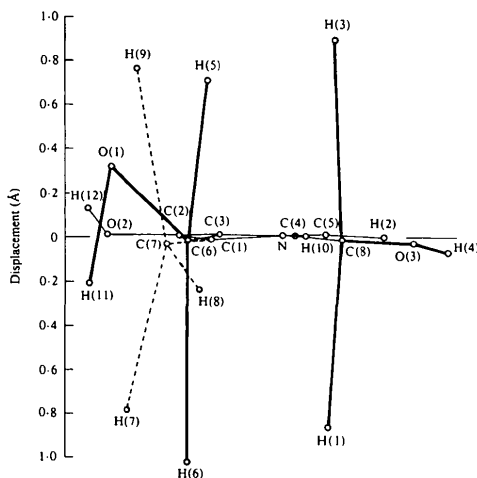
group is twisted internally in so far as OH is asymmetric with respect to CH<sub>2</sub>, as represented by an inequality between dihedral angles 22.0 (7)° and 97.7 (7)° in Table 4. On the other hand, O(3)—H(4) of the other CH<sub>2</sub>OH group is symmetric with CH<sub>2</sub>, as represented by dihedral angles 57.0 (8), 62.1 (8)°, and lies quite close to the molecular plane. The distinction between the two CH<sub>2</sub>OH groups is made clear in Fig. 2, which indicates displacements of atoms from a plane fitted through the core of the pyridoxinium molecule. Each individual molecule is flat, apart from hydrogen atoms of CH<sub>3</sub>, CH<sub>2</sub>OH, OH and the CH<sub>2</sub>OH oxygen atom O(1), which takes part in the intramolecular bond. Displacements are listed in Table 5. Fig. 2 greatly

Table 4. *Torsion angles (°) based on nuclear positions as determined with neutrons*The top portion of the table contrasts dihedral angles for the two different CH<sub>2</sub>OH groups.

C(4)–C(8)–O(3)–H(4)	178.0 (6)	C(3)–C(6)–O(1)–H(11)	-142.6 (5)
C(3)–C(4)–C(8)–O(3)	-179.1 (3)	C(4)–C(3)–C(6)–O(1)	-165.4 (3)
C(5)–C(4)–C(8)–O(3)	1.2 (4)	C(2)–C(3)–C(6)–O(1)	16.5 (4)
C(5)–C(4)–C(8)–H(3)	-120.6 (6)	C(2)–C(3)–C(6)–H(5)	135.8 (6)
C(5)–C(4)–C(8)–H(1)	124.8 (5)	C(2)–C(3)–C(6)–H(6)	-105.3 (5)
H(1)–C(8)–O(3)–H(4)	57.0 (8)	H(6)–C(6)–O(1)–H(11)	-22.0 (7)
H(3)–C(8)–O(3)–H(4)	-62.1 (8)	H(5)–C(6)–O(1)–H(11)	97.7 (7)
C(2)–O(2)–H(12)–O(1)	0.9 (1.3)	C(1)–C(2)–C(3)–C(4)	-0.1 (4)
O(2)–H(12)–O(1)–C(6)	12.8 (1.2)	C(2)–C(3)–C(4)–C(5)	-1.2 (4)
H(12)–O(1)–C(6)–C(3)	-17.3 (4)	C(3)–C(4)–C(5)–N	1.4 (4)
O(1)–C(6)–C(3)–C(2)	16.5 (4)	C(4)–C(5)–N–C(1)	-0.2 (4)
C(6)–C(3)–C(2)–O(2)	-2.0 (5)	C(5)–N–C(1)–C(2)	1.1 (4)
C(3)–C(2)–O(2)–H(12)	-6.6 (6)	N–C(1)–C(2)–C(3)	1.2 (4)
H(12')–O(2')–H(12)–O(2)	0.0 (6)	C(1)–C(2)–C(3)–C(6)	178.0 (3)
O(2')–H(12)–O(2)–H(12')	0.0 (3)	C(5)–C(4)–C(3)–C(6)	-179.4 (3)
H(12')–O(2')–H(12)–O(1)	-178.9 (6)	C(2)–C(3)–C(4)–C(8)	179.1 (3)
O(2')–H(12)–O(2)–C(2)	-177.4 (3)	N–C(5)–C(4)–C(8)	-179.0 (3)
O(2')–H(12)–O(1)–C(6)	-169.2 (3)	C(3)–C(4)–C(5)–H(2)	179.1 (5)
O(2')–H(12)–O(1)–H(11)	-47.6 (7)	C(1)–N–C(5)–H(2)	-178.1 (5)
N–C(1)–C(7)–H(7)	-129.7 (7)	C(4)–C(5)–N–H(10)	178.5 (4)
N–C(1)–C(7)–H(8)	-11.5 (8)	C(2)–C(1)–N–H(10)	-179.8 (4)
N–C(1)–C(7)–H(9)	121.3 (7)	C(5)–N–C(1)–C(7)	179.0 (3)
C(1)–C(2)–O(2)–H(12)	173.3 (5)	C(3)–C(2)–C(1)–C(7)	-178.9 (3)
		N–C(1)–C(2)–O(2)	-178.8 (3)
		C(4)–C(3)–C(2)–O(2)	179.9 (3)

Table 5. *Displacements (Å) from fitted plane ( $-0.1569x + 0.5555y + 0.8166z = 1.6782$ ) through nuclear positions in CO core of single molecule*

Atoms in fitted plane				Other atoms			
C(1)	0.007 (3)	C(6)	0.016 (3)	H(6)	1.020 (7)	H(8)	0.235 (11)
C(2)	-0.008 (3)	C(7)	0.037 (3)	H(5)	-0.711 (8)	H(7)	0.789 (12)
C(3)	-0.013 (3)	C(8)	0.010 (3)	O(1)	-0.323 (3)	H(9)	-0.765 (10)
C(4)	-0.005 (3)	O(2)	-0.017 (4)	H(11)	0.208 (6)	H(12)	-0.139 (6)
C(5)	-0.017 (3)	O(3)	0.037 (4)	H(1)	0.859 (8)	H(2)	-0.002 (6)
N	-0.009 (2)			H(3)	-0.882 (8)	H(10)	-0.005 (6)
				H(4)	0.077 (7)	Cl	-0.153 (2)
						Cl'	0.171 (2)

Fig. 2. Displacements of atoms from a plane fitted through the core of a pyridoxinium ion. The scale for the vertical axis is magnified four times more than that for the horizontal axis. The two CH<sub>2</sub>OH groups are outlined with bold lines, and CH<sub>3</sub> with broken lines, to aid identification.

exaggerates these displacements, as its vertical scale is magnified fourfold relative to that of the horizontal axis.

### Rigid-body motion

Rigid-body analyses of the thermal motion were made first by constraining only a skeleton of atoms, at the core of each pyridoxinium ion, to move as a rigid group. In the first instance, only a central C<sub>8</sub>NO frame of atoms was constrained in this way and the remaining atoms were allowed to move individually. This gave rise to 0.0020 Å<sup>2</sup> r.m.s. for an *R* of agreement  $\Delta(U)$  between the thermal motion of the assumed rigid frame and the  $U_{ij}$ , as listed in Table 1, of those particular atoms that were taken to be a part of the rigid group. The librations 5.3, 2.8, 2.1° r.m.s. and translations 0.18, 0.14, 0.17 Å r.m.s. obtained from this analysis can be compared with further values 4.7, 2.5, 1.3° r.m.s. and 0.18, 0.14, 0.17 Å r.m.s.: these latter values arise from an analysis that places rigid constraints also

on the two remaining O atoms, belonging to the two  $\text{CH}_2\text{OH}$  groups, thus forming a slightly enlarged rigid frame  $\text{C}_8\text{NO}_3$ , instead of  $\text{C}_8\text{NO}$ . It should be noted however that the discrepancy factor  $\Delta(U)$  then increased markedly from 0.0020 to 0.0035  $\text{\AA}^2$  r.m.s.

Both of these analyses indicate a motion that is largely isotropic, except that the molecular core librates most about an axis across the flat strips of adjoining molecules, whilst the smallest molecular libration is about an axis roughly along the length of the strip. It may be noted that the largest libration occurs about an axis that roughly coincides with the one that has the lowest moment of inertia, if it is assumed that the individual molecules are effectively unlinked. The largest librational component can be pictured in the form of a transverse standing wave, such that the largest amplitudes of displacement lie perpendicular to the plane of the flat strip. Flexible hinges can be considered to operate in this strip, near the planar  $\text{O}-\text{H}\cdots\text{O}$  and  $\text{Cl}$  linkages at the ends of each molecule, such that the maximum amplitudes of displacement occur near these 'hinges'.

When similar analyses were conducted on a bimolecular pair (Fig. 1), much smaller values 0, 0,  $0^\circ$  r.m.s. were obtained for the librations of a dimer. Furthermore, the average discrepancy factor  $\Delta(U)$  rose from 0.0020  $\text{\AA}^2$  r.m.s. to 0.0069  $\text{\AA}^2$  r.m.s., for a dimer

pair  $(\text{C}_8\text{NO})_2$  of molecular cores. This is consistent with the notion that the dimer is not in fact rigid. It would appear that flexings and stretchings occur at *both* ends of each molecule, not least at the centre of the bimolecular pair.

Further analyses were made of the motion of each individual molecule. In these more ambitious analyses, all the atoms in each molecule, except extreme ones  $\text{Cl}$ ,  $\text{H}(4)$ ,  $\text{H}(11)$ , were constrained to move as a single rigid group, with a concession that certain side groups could *also* librate about their  $\text{C}-\text{C}$  links to the pyridine ring. This gave rise, with a  $\Delta(U)$  of 0.0134  $\text{\AA}^2$  r.m.s., to rather similar molecular librations 4.2, 3.5, 2.8° r.m.s. and translations 0.20, 0.14, 0.17  $\text{\AA}$  r.m.s. as above, together with 6, 9, 25° r.m.s. respectively for the libration of those particular side groups  $\text{H}_2\text{C}(6)\text{O}(1)$ ,  $\text{H}_2\text{C}(8)\text{O}(3)$ ,  $\text{CH}_3$ , that were allowed to oscillate about their  $\text{C}-\text{C}$  links to the pyridine ring. It seems reasonable that the group  $\text{H}_2\text{C}(6)\text{O}(1)$  is found to librate less than  $\text{H}_2\text{C}(8)\text{O}(3)$ , in view of its intramolecular bonding of  $\text{O}(1)$  to  $\text{H}(12)$  (see Fig. 1). A large  $\text{CH}_3$  libration in particular is apparent in the thermal ellipsoids of Fig. 1.

The thermal librations, affecting the mean atomic positions, lead to shortening of the bond lengths and a correction for this effect is indicated in Table 2.

#### Comparison of X-ray and neutron results

The results labelled 're-assessed X-ray' in Tables 2 and 3 arise from a repeat refinement of the structural parameters, using Hanic's X-ray data, starting from the neutron results of Table 1. The hydrogen 1s electron clouds (Stewart, Davidson & Simpson, 1965) were assumed to be fully filled and have thermal parameters fixed at values (Table 1) which were determined by neutrons for their nuclei. The crystallographic  $R(F)$  factor fell from an initial value 17.2 to 9.7%. Whilst estimated standard deviations are large for the deduced mean positions of the hydrogen electron clouds, the re-assessed X-ray results for other constituent atoms of this compound are sufficiently accurate (Table 2) to display a general expansion of bond lengths, beyond Hanic's values, that can be attributed to the present revision of crystal cell dimensions. Quantities that involve  $\text{H}(4)$ ,  $\text{H}(5)$ ,  $\text{H}(7)$  and  $\text{H}(12)$  are omitted from the 're-assessed X-ray' list of values in Tables 2 and 3, as each of these atoms meandered by more than an ångström from its starting position, in the present re-appraisal of the X-ray data, with little or no effect on crystallographic  $R$  factors. The remaining hydrogen atoms did not move so far from their neutron-determined positions, except  $\text{H}(11)$  which shifted about 0.5 (1)  $\text{\AA}$ , roughly towards an adjacent  $\text{Cl}$  atom.

Fig. 3 illustrates a more detailed comparison between the available X-ray and neutron data. This  $X-N$  difference-Fourier map represents a difference between

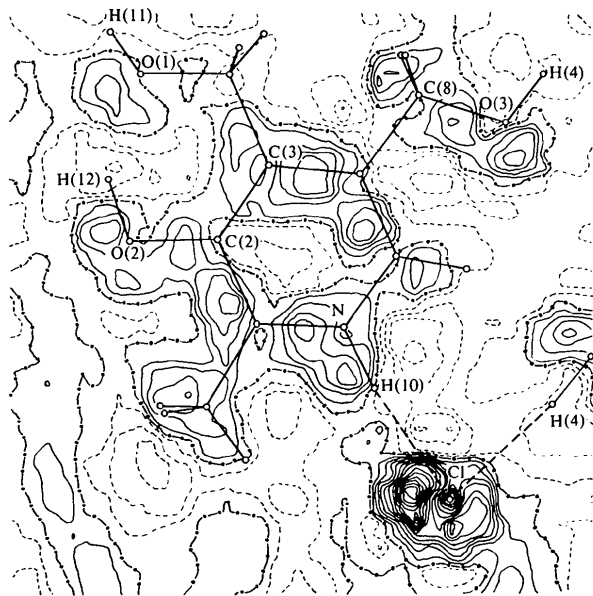


Fig. 3. Bonding electron density, as deduced by  $X-N$  difference-Fourier technique, in the plane described in Table 5 as fitted through the core of the pyridoxinium ion. In the immediate vicinity of the  $\text{Cl}$  atom, the electron density falls steeply, reaching a minimum value in this plane of  $-0.6 \text{ e \AA}^{-3}$ , but no negative contours are drawn here, for reasons of crowding. Otherwise, contours are drawn at every  $0.1 \text{ e \AA}^{-3}$ . Negative contours are dashed, zero contours are chained and positive contours are drawn as full lines.

electron density, as determined with X-rays, and that which would arise from 'free' spherical atoms placed at the nuclear positions determined with neutrons. A relevant scale factor was refined using Hanic's X-ray data and the neutron-determined (Table 1) structural parameters. Surfeits of electron density can be seen in Fig. 3 near the marked positions of all three oxygen nuclei and these may be attributed to 'lone pair' electron density. In particular, this excess density for O(2) is placed about the *intermolecular* bond O(2)···H(12) such that it impinges upon the path of O(2)—H(12). This, together with an apparent deficit of electrons in Fig. 3 around the marked position of the H(12) proton, could explain the possibility of obtaining a short value for the O(2)—H(12) bond lengths with X-rays. Indeed, Hanic (1968) placed the centre of the H(12) electron cloud 0.2 Å nearer O(2) than the present neutron-determined position of its proton. The magnitude of this discrepancy between neutron and X-ray scattering centres is similar to that found for hydrogen atoms in other compounds, such as in  $\alpha$ -oxalic acid dihydrate and *sym*-triazine (Coppens, Sabine, Delaplane & Ibers, 1969).

Fig. 3 displays surfeits of electron density near the middle of most bonds, as well as near the electro-negative Cl atom. The maximum surfeit of electron density in Fig. 3 occurs near the Cl atom and equals  $1.4 \text{ e } \text{Å}^{-3}$ , which is about 10% of the full density arising at that point. The maximum excess electron density in the pyridine ring is  $0.6 \text{ e } \text{Å}^{-3}$ , which is about 10% of the maximum full density arising at the centre of each C atom. There is hardly any significant evidence, however, that excess electrons congregate near the N atom of the pyridine ring, any more than near C(3) for example.

In a further re-assessment of Hanic's X-ray data, all the atomic parameters were fixed at their neutron-

determined values (Table 1) and site-occupancy factors alone were refined, just for the hydrogen atoms. This gave rise to a slight decrease in  $R(F)$  from 17.2 to 17.0% and to occupancy values 1.2 (1), 0.7 (1), 1.1 (1), 0.4 (1), 0.7 (1), 0.4 (1), 1.2 (1), 0.5 (1), 0.0 (1), 0.9 (1), 0.9 (1), 0.4 (1) for the atoms H(1) to H(12). Although any detailed attempt at interpretation of these results seems inappropriate, there is a general indication that the hydrogen atoms do not all possess a whole 1s electron. For example, H(4) and H(12), which moved appreciably in the present X-ray positional re-appraisal, have assumed condensed 1s electron clouds that seem, on the basis of this re-assessment, to be less than half full.

We are grateful to the Science Research Council and the Institut Laue-Langevin for providing the means of carrying out these experiments and the former for supporting one of us (JSP) with a postdoctoral award during the early stages of this work.

#### References

- COPPENS, P., SABINE, T. M., DELAPLANE, R. G. & IBERS, J. A. (1969). *Acta Cryst.* **B25**, 2451–2458.  
 HANIC, F. (1966). *Acta Cryst.* **21**, 332–340.  
 HANIC, F. (1968). *Chem. Zvesti.* **22**, 838–843.  
 JOHNSON, C. (1970). *ORTEP*. Report ORNL-3794. Oak Ridge National Laboratory, Tennessee.  
 SHELDRICK, G. M. (1976). *SHELX 76*. A program for crystal-structure determination. Univ. of Cambridge, England.  
 STEWART, R. F., DAVIDSON, E. R. & SIMPSON, W. T. (1965). *J. Chem. Phys.* **42**, 3175–3187.  
 XRAY 72 (1972). Computer Science Center, Univ. of Maryland, College Park, Maryland.

*Acta Cryst.* (1980). **B36**, 1136–1141

## A Comparison of the Structures of Three Substituted 2-Benzoylpyrroles

BY ROBIN B. ENGLISH,\* GEORGE MCGILLIVRAY AND IN PART ELMA SMAL

*Department of Chemistry, University of South Africa, PO Box 392, Pretoria, South Africa*

(Received 1 November 1979; accepted 2 January 1980)

#### Abstract

The structures of 2-benzoylpyrrole (BZP), 2-(4-chlorobenzoyl)pyrrole (CLBZP) and 2-(4-methoxybenzoyl)-

pyrrole (MEBZP) are described. BZP crystallizes in space group  $P1$  with  $a = 10.687(5)$ ,  $b = 10.623(5)$ ,  $c = 3.953(5)$  Å,  $\alpha = 98.35(1)$ ,  $\beta = 98.38(1)$ ,  $\gamma = 98.11(1)^\circ$ ,  $Z = 2$ . CLBZP and MEBZP crystallize in space groups  $P2_1/n$  and  $P2_1/c$  respectively: for CLBZP  $a = 11.760(5)$ ,  $b = 21.077(5)$ ,  $c = 3.919(5)$

\* To whom correspondence should be addressed.